Behavior of RCS Connections with Void Web Under Cyclic Load Reversals

Yudi Herdiansah[1, 2*], Bambang Budiono[3], Herlien D. Soemari [3] & Indra Djati Sidi[3]

[1]Post-Graduate Program of Civil Engineering Department
Faculty of Civil and Environmental Engineering, Bandung Institute of Technology
Jalan Ganesha No. 10, Bandung 40132, Indonesia
[2]Civil Engineering Department, Faculty of Engineering, University of Jenderal Achmad Yani, Jalan Terusan Jenderal Sudirman PO. BOX. 148, Cimahi 40531, Indonesia
[3]Structure Research Group, Civil Engineering Department,
Faculty of Civil and Environmental Engineering, Bandung Institute of Technology
Jalan Ganesha No. 10, Bandung 40132, Indonesia
*E-mail: yudi.herdiansah@lecture.unjani.ac.id

Highlights:

- A new RCS joint detail with a void web and EBP was developed to solve constructability issues in RCS connections.
- A void web on RCS beam-column connections has no significant effect on reducing the capacity/strength of the connection.
- EBP has proven to be very effective in providing confinement and reducing the level of damage in the joint panel.

Abstract. In this study, the inelastic cyclic behavior of hybrid connections consisting of reinforced concrete column and steel beams (RCS) was investigated. The experimental results from the lateral load testing of four interior RCS subassembly connections are presented. The first specimen was designed based on the *ASCE Guidelines 1994*, with connection details based on the study of Liang and Parra-Montesinos (2004), while another specimen was a proposed joint detail. The joint detail was developed to overcome the main problems with RCS frame systems, which is constructability. The behavior of the beam-column joints was evaluated in terms of strength capacity, stiffness degradation, energy dissipation, and joint shear distortion. Comparing all specimens based on the load-displacement hysteresis curves indicated that the specimen with the combination of ABP and EBP had relatively better performance in terms of strength, stiffness, and energy dissipation. ABP and EBF in the joint with a void web were able to withstand joint shear deformation exceeding 0.01 rad, with only low to medium level of damage. EBF was proven to be very effective in providing confinement and reducing the damage level in the joint panel. The existence of a void web did not affect the reduction of joint shear strength.

1   Introduction

In the last three decades, a new structural system called reinforced concrete steel (RCS) has been developed. RCS is a moment-resisting frame system consisting of steel beams and reinforced concrete columns. RCS systems combine the advantages of concrete and steel to form an efficient structural system. Reinforced concrete columns to replace steel columns can save costs and increase the lateral stiffness of the structure and the capacity to withstand compressive axial loads. In addition, a composite floor system with steel beams is lighter than a reinforced concrete floor system, thereby reducing the weight and inertia of the structure. A typical detail of an RCS joint is shown in Figure. 1.
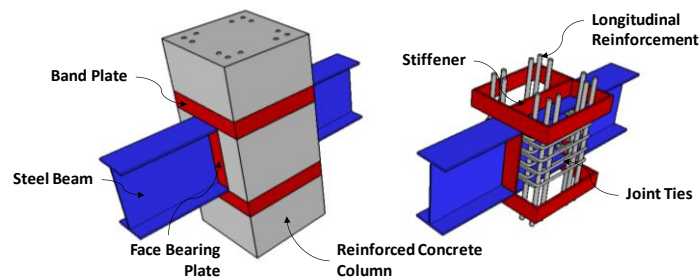
Figure 1 Typical detail of an RCS joint.

The first and most important study of the RCS connection was conducted at the University of Texas, Austin by Sheikh, *et al*. in [1] and Deierlein, *et al*. in [2]. Fifteen beam-column joint specimens at 2/3 scale were tested to quantify joint strength and stiffness in various details, including face bearing plates (FBP), extended face bearing plates (E-FBP), inset bearing plates (IBP), steel columns, shear studs, and vertical bars. Sheikh, *et al*. in [3] and Deierlein, *et al*. in [4] divide the behavior of the joints into two failure modes: (1) panel shear failure, shown by significant diagonal cracks in the concrete panel and yielding of the steel web panels in the joint area; and (2) vertical bearing failure, shown by concrete crushing at the top and bottom of the steel beam flanges. The results of these studies were the basis for ASCE design recommendations for beam-column moment connections in composite frames (ASCE 1994) [5]. After ASCE 1994 was published several studies have been conducted to further develop the RCS system, including those related to (1) validation and development for use in high seismic zones; (2) reducing the need for transverse reinforcement in the connection panel; (3) standard models to accommodate more varied connection details; (4) modifications to differentiate between interior and exterior connections; (5) the use of high-strength concrete. From these studies, only a few have developed new connection details to improve RCS connection constructability, especially for application in precast systems. Some of the

researchers who conducted studies to improve the constructability of the RCS system are Cordova and Deierlein, *et al*. [6]. They conducted a full-scale test that, among others, was aimed at investigating the seismic performance and constructability of the RCS moment-resisting frame. Alizadeh, *et al*. in [7] investigated new connection details using self-consolidating concrete (SCC) to facilitate the constructability of the RCS system.

2 Research Objectives

One of the main problems of the RCS system is constructability. This occurs because the ratio of steel to concrete volume in the joint region is quite large due to the existence of continuous steel beams, longitudinal reinforcement of columns, and joint stirrups. Construction difficulties occur during the concrete casting process. RCS with continuous beams has high potential to form air cavities trapped between the beams and the FBP in the joint region. The potential for trapped air cavities is greater in RCS precast production, which is generally done by casting in a lying position. Removing most of the steel web plates on the joint panel (void web) can reduce this potential.

This paper presents the result of an investigation that includes the testing of four RCS beam-column subassemblies under cyclic loading. The objectives of this research were to investigate the application of new connection details to solve the constructability problem with RCS connections, especially for precast systems. A new connection detail, consisting of a void web combined with additional bearing plates (ABP), band plates, extended band plates (EBP), and U-shape stirrups, was developed to improve the seismic performance. The behavior of the connections was evaluated in terms of strength and distortion, stiffness degradation, energy dissipation capacity, and drift components.

3 Experimental Study

The experimental program was divided into two stages. Stage 1 involved Specimens 1 and 2, which were planned as preliminary tests to evaluate the potential of the new connection details, which consisted of a void web, ABP, EBP, and U-shape stirrups. The second stage involved specimens 3 and 4, to evaluate the effect of each EBP, ABP, and stirrup volume ratio to the overall behavior of the RCS beam-column joint.

3.1 Test Specimens

The test specimens were four ¾-scale interior RCS beam-column subassembly connections with continuous beams. The column design referred to the Building Code Requirements for Structural Concrete (ACI 316M-14) [8] for special
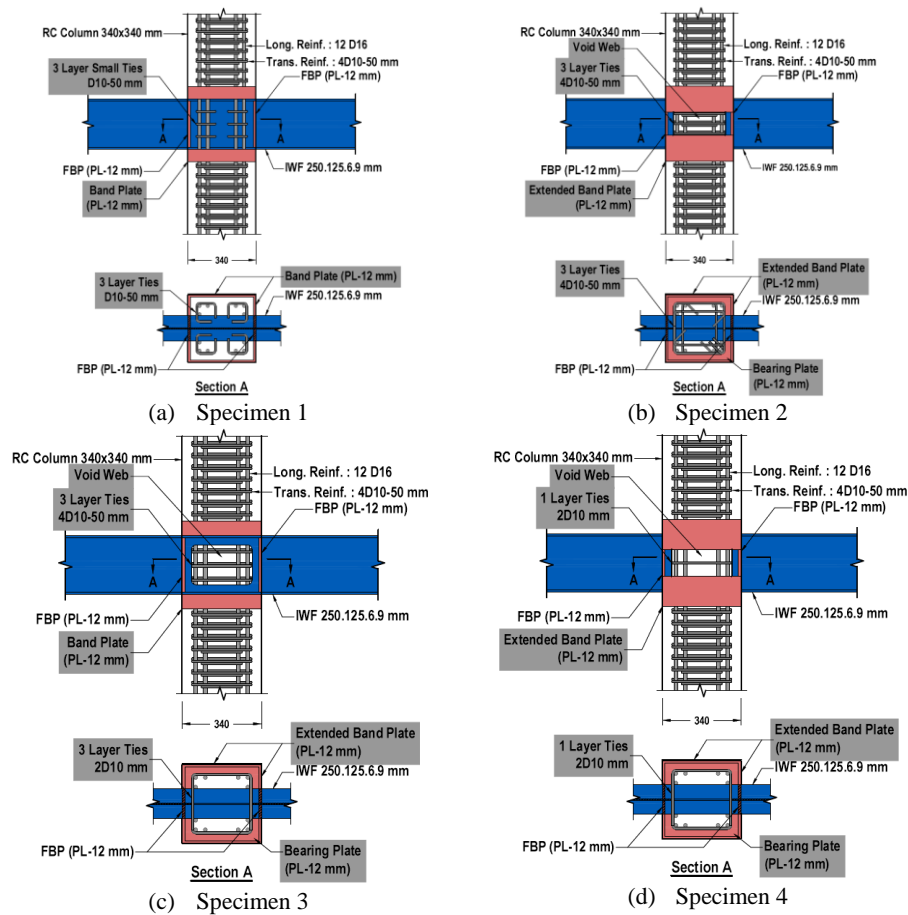
moment frames. Square columns with a cross-section of 340×340 mm^2 were used for all specimens. The longitudinal column reinforcement consisted of 12 deformed bars of 16 mm in diameter (12 D16), representing approximately 2.09% of the gross column area. The concrete columns had a mean compressive strength approximately of 45 MPa for all specimens, with a maximum coarse aggregate size of 10 mm. In this research, the beams were designed as non-composite in accordance with the Seismic Provisions for Structural Steel Buildings (ANSI/AISC 341-16) [9]. The structural steel beams for all specimens were IWF 250 x 125 x 6 x 9 with A36 steel based on ASTM A572 [10]. The beams were designed as highly ductile structural elements. In addition, the strong column – weak beam philosophy was adopted in the design of the specimens along with a column-beam actual moment strength ratio of approximately 1.6.

Specimen 1 was designed based on the ASCE Guidelines 1994 with connection details based on the study of Liang and Parra-Montesinos [11]. Specimen 1 was used as a reference to be compared with the other proposed specimens. Specimen 1 consisted of a small stirrup to tie the longitudinal reinforcement, as has been studied by Liang and Parra-Montesinos, while for Specimen 2, U-shape stirrups were used that crossed through a steel void web at the panel joint. These stirrups were expected to contribute to increasing the joint shear strength and provide confinement to the concrete in the connection area. An EBP was placed in Specimen 2 with the same thickness as the band plates in Specimen 1, i.e. 12 mm. In Specimen 2, a 12-mm thick ABP was welded to the steel beam flange and an EBP was attached on each side of the joint. The ABP was attached to the joint region to increase the bearing and shear strength of the joint. An FBP with the same width as the steel beam flange was attached to all specimens.

Specimen 3 was designed almost the same as Specimen 1, with the connection details consisting of band plates and an FBP, both with a thickness of 12 mm. The differences between Specimen 3 and Specimen 1 were that Specimen 3 was installed with a 12-mm thick ABP and there was a void web in the connection area. Three layers of 2-foot U-shaped hoops with a diameter of 10 mm were installed with 50-mm spacing to the void web. Specimen 4 was designed to be the same as Specimen 2, with identical component dimensions of the connection detailing. The only difference between Specimen 4 and Specimen 2 was the number of stirrups installed in the connection area. In Specimen 4, only one layer of 2-foot U-shaped hoops with a diameter of 10 mm was installed so that the stirrup volume ratio was smaller than that of Specimen 2. Based on a comparison of those two specimens, the effect of the stirrup ratio on the connection behavior could be evaluated. The specimen details and dimensions for the experimental studies are shown in Table 1 and Figure 2.

Table 1   Experimental program.

Component			Specimen			
			1	2	3	4
Connection Details	*Additional Bearing Plate* (ABP)	Thickness	-	12 mm	12 mm	12 mm
		Width	-	38 mm	38 mm	38 mm
	Band Plate (BP)	Thickness	12 mm	-	-	12 mm
		Height	62,5 mm	-	62,5 mm	-
	Extended Band Plate (EBP)	Thickness	-	12 mm	-	12 mm
		Height	-	129,5 mm	-	129,5 mm
	Face Bearing Plate (FBP)	Thickness	12 mm	12 mm	12 mm	12 mm
		Width	125 mm	125 mm	125 mm	125 mm
	Void Web		-	(260 x 170) mm²	(260 x 170) mm²	(260 x 170) mm²
	Ties in Joint Panel		3 Layer Small Ties D10-50 mm	3 Layer Ties 4D10-50 mm	3 Layer Ties 2D10	1 Layer Ties 2D10
	Volumetric Ratio of Ties		1,20%	1,50%	0,85%	0,28%
Beam	Section		IWF 250x125x6x9			
Column	Section		340x340 mm			
	Long. Reinf.		12 D16 ($r_g = 2,09\%$)			
	Trans. Reinf.		4 D10-50 mm ($r_w = 1,85\%$)			
	Axial Load		462,4 kN (= 0,1 f_c' A_g)			

(a)   Specimen 1

(b)   Specimen 2

(c)   Specimen 3

(d)   Specimen 4

Figure 2   Specimen details.

3.2   Test Setup, Loading Pattern and Instrumentatio

The test setup used for the experimental program is shown in Figure 3. All columns and beams were connected to a pin support at each end to represent the inflection points at the member midspan. Lateral cyclic displacement was applied at the top of the column through a 1000 kN hydraulic actuator attached to a strong wall.
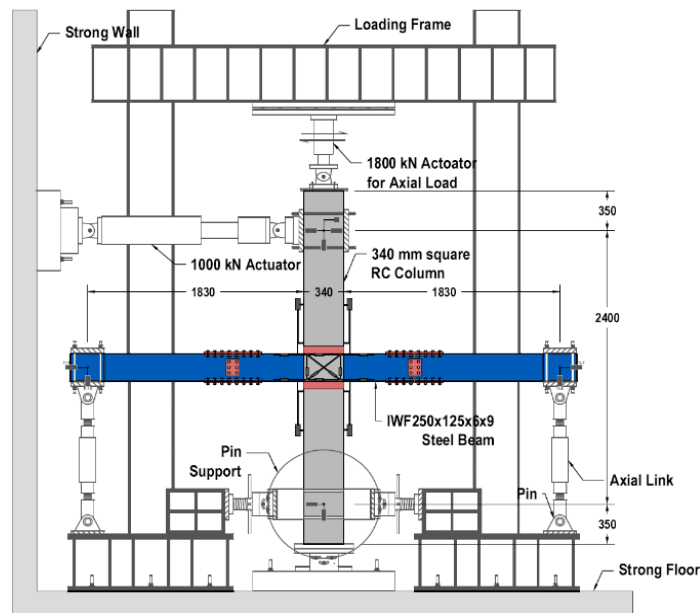

Figure 3 Test setup.

Axial load was applied to the column at approximately 462.4 kN to simulate the minimum axial load, i.e. about 10% of the column's axial gross strength, through an 1800 kN hydraulic actuator attached to a loading frame. A load cell and displacement transducer were used to monitor lateral loads and displacements applied at the top of the column. A displacement transducer was placed near the bottom of the column to monitor the slip occurring in the instrument setup. The actual slip was obtained by reducing the lateral displacement applied with the displacement occurring at the bottom of the column. The displacement transducer was also used to measure joint deformation and beam rotation.

Twenty-two lateral displacements were applied to the specimen, with displacement amplitudes ranging from 0.5% to 6.0% of the story drift ratio. Each loading cycle was repeated once to evaluate the degradation of stiffness and strength. The loading pattern referred to ANSI/AISC 341-10 and ACI 374.2R-13 [9]. The displacement load pattern is shown in Figure 4.
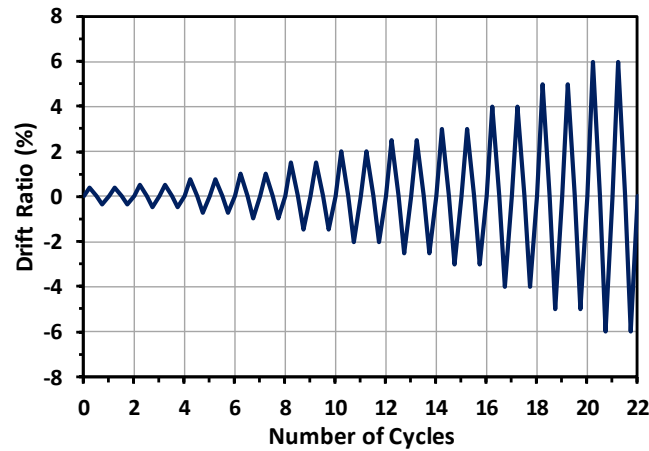
Figure 4 Lateral loading pattern.

4 Results

4.1 Cyclic Behavior and Crack Pattern

The lateral load versus story drift response for all specimens is shown in Figure 5. All four specimens showed stable lateral load versus story drift behavior. Specimen 1 was tested as the benchmark for all other specimens with the proposed detail connection. In stage 1 of the experiment, first diagonal cracks at the joint panel in Specimen 1 occurred at 1.0% story drift along with flexural cracks observed in the concrete column. Cracks in the elastic range occurred until 1.0% story drift and then the steel beam started to yield at the flange near the edge of the column. Significant yield on the beam was observed when the story drift reached 4.0% and local buckling began to occur on the top and bottom steel beam flange.

Most of the cracks in the joint panel occurred before the drift ratio reached 4.0%. Band plates attach to Specimen 1 provided good restraints, thus minimizing the occurrence of bearing cracks that may occur in the interface between the steel beam and the concrete column. Cracks at the edge of the band plate occurred at 5.0% story drift; these cracks were closed during unloading, thus minimizing rigid body rotation of the beam in the joint region.

The first diagonal cracks in Specimen 2 appeared at 1.0% drift ratio, while the first flexural cracks in the column occurred when the story drift reached 0.75%. Cracks in the elastic range occurred at 1.0% story drift, after which the steel beam started to yield at the flange near the edge of the column. Unlike Specimen 1,

significant yield occurred in Specimen 2 at the beam flange when the story drift reached 5.0%, characterized by the beginning of local buckling on the top and bottom beam flanges.
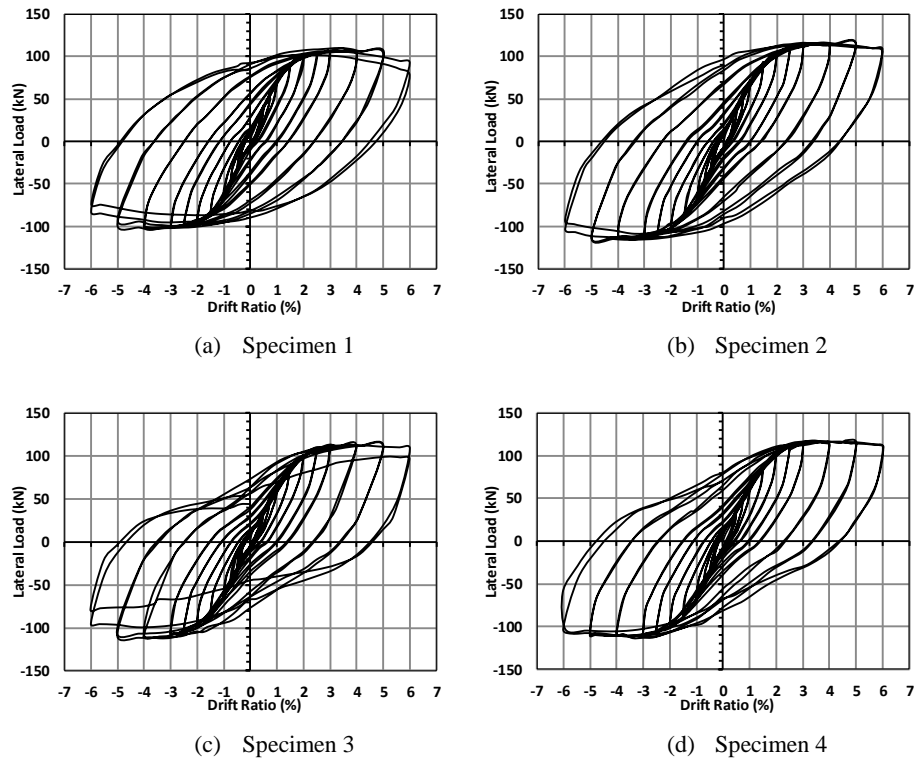

(a) Specimen 1   (b) Specimen 2

(c) Specimen 3   (d) Specimen 4

Figure 5 Lateral load versus drift ratio response.

Most cracks in the joint region occurred before 4.0% story drift. EBP and ABP used in Specimen 2 provided excellent confinement, preventing the occurrence of diagonal cracks in the joint concrete panel and also bearing cracks that may occur in the interface between the steel beams and the concrete columns. No cracks appeared at the edge of the EBP until 6.0% drift ratio. In stage 1, Specimens 1 and 2 showed low to medium damage levels. Most of the inelastic deformation occurred in the steel beams, based on the strong column – weak beam design criteria. The crack patterns in all specimens at 6.0% drift ratio at the end of the test are shown in Figure 6.

From the second stage of the experiment, the first diagonal cracks in the joint panel of Specimens 3 and 4 appeared at 0.75% story drift, and flexural cracks in the column were first detected when the story drift reached 1.0%. The steel beams

started to yield at 1.0% story drift at the flange near the face of the column. In Specimen 3, cracks at the edges of BP occurred at 2.0% story drift, while in Specimen 4, cracks at the edges of EBP were detected at 1.5% story drift.
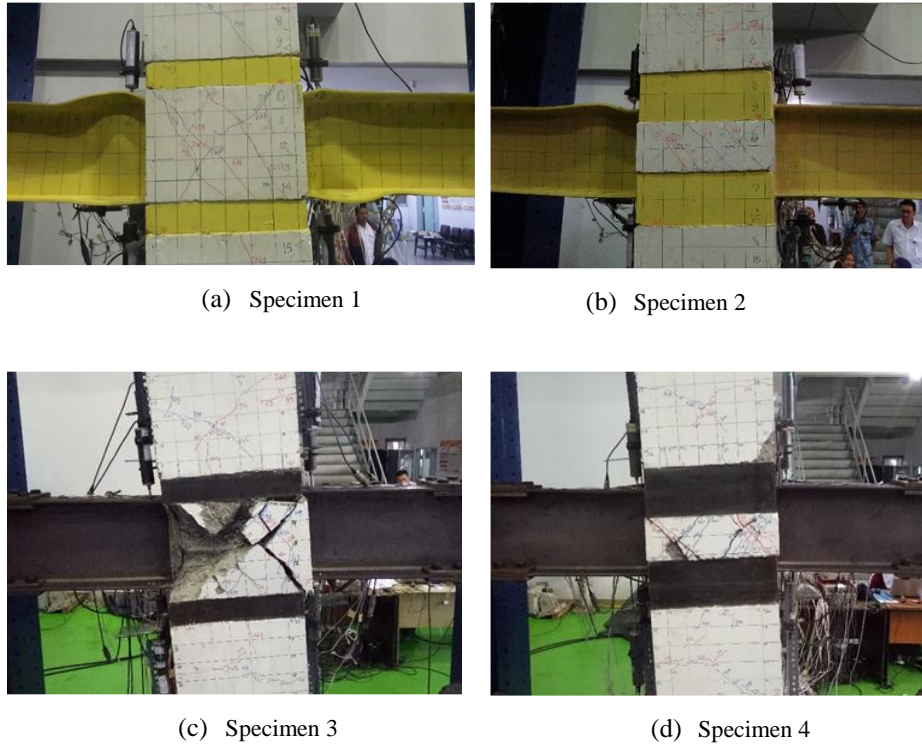

(a) Specimen 1   (b) Specimen 2

(c) Specimen 3   (d) Specimen 4

Figure 6 Joint cracking and beam yielding in the test specimens at the end of test.

The cracks tended to enlarge with increasing drift ratio and closed during the unloading process. Local buckling at the flange near the face of the column appeared along with significant yield in the beam, which occurred at 4.0% and 5.0% story drift for Specimens 3 and 4. However, only insignificant local buckling occurred, unlike what happened in Specimens 1 and 2.

Most of the cracks in Specimen 3 and 4 occurred before reaching 4.0% story drift. In Specimen 3, significant damage occurred in the connection panel area at the end cycle of 6.0% story drift. This damage was marked by concrete spalling until the stirrups in the connection panel were exposed, as shown in Figure 6(c). The damage was also characterized by buckling in the FBP, caused by pressure from the concrete compressive strut on the joint panel.

4.2 Strength Capacity

The strength capacity of each specimen was evaluated from the backbone curves of load versus displacement formed by connecting the peak points of the hysteresis curves, as shown in Figure 7.

The maximum strength in Specimen 1 was achieved at a drift ratio of 4.0%. At positive load, the strength remained stable until 5.0% drift ratio and decreased at 6.0% drift ratio due to significant local buckling in the steel beam flange, whereas under negative load a decrease at 5.0% drift ratio was observed. Compared to the other specimens, the strength of Specimen 1 was smaller due to the local buckling of the steel beam flange identified at 2.0% drift ratio, which became significant when reaching maximum load, leading to a decrease in strength.
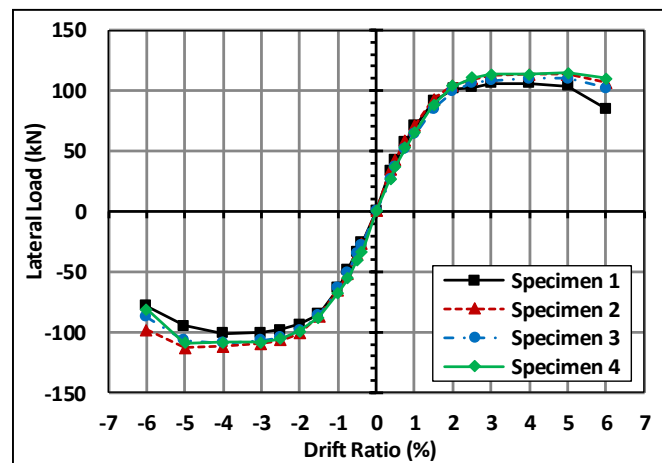

Figure 7 Lateral load versus drift ratio envelope.

In Specimens 2 and 4, maximum strength occurred at 5.0% drift ratio and strength increased by 8-9.5% compared to Specimen 1. That is due to the high level of restraint on the concrete panels at the joint provided by the EBP and the ABP, thereby increasing the strength of the concrete compressive strut. The strength remained stable up to 6.0% drift ratio, while under negative load the strength of Specimen 4 decreased at 6.0% drift ratio.

The maximum load in Specimen 3 was reached in the first cycle at drift ratio 4.0% and remained stable until drift ratio 5.0%. A significant load decrease relative to the other specimens occurred at 6.0% drift ratio under negative load. The increase in peak load of Specimen 3 against Specimen 1 was 4% and 8% for positive and negative load. The effect of the EBP can be seen by comparing Specimens 3 and 4, where the latter has an EBP while the former does not.

Specimens 3 and 4 had relatively similar strength. A difference was only seen in the final loading cycle, where more significant strength degradation occurred in Specimen 3 at 6.0% drift ratio.

4.3   Stiffness Capacity

A stiffness comparison of the specimens is displayed in the form of a peak-to-peak stiffness degradation curve. Stiffness degradation is the process of losing structural stiffness at each loading cycle. Peak-to-peak stiffness of each loading cycle is based on the slope of the line from the positive peak load point to the negative peak load point. A comparison of peak-to-peak stiffness for each specimen can be seen in Figure 8.

From that figure it can be seen that Specimen 2 had the best stiffness retention capacity for each loading cycle, with insignificant differences. This shows that the proposed connection details in Specimen 2 had relatively better stiffness, contributing to an increase in overall structural stiffness. Detailing with ABP and EBP coupled with stirrups in adequate connection areas is quite effective in increasing the stiffness of the connection panel, thereby increasing the overall structural stiffness.
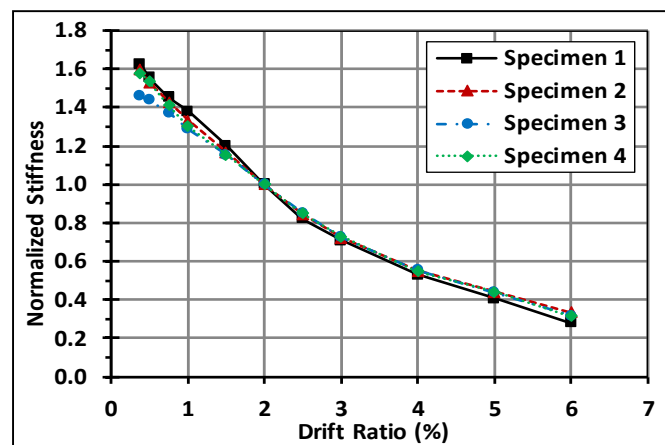

Figure 8 Normalized stiffness versus drift ratio.

The stiffness of Specimen 3 was relatively small compared to that of the other specimens at a low drift ratio, i.e. between 0.375% to 1.50%. This was due to the occurrence of diagonal cracks in the initial stages of loading with relatively large crack sizes. These cracks were the result of insufficient stirrups in the connection area (see Figure 6(c)). No restraint can prevent the outer concrete panel joint from crack magnification and there is potential for slip between the outer concrete

panel with ABP, which can magnify the crack. At a drift ratio greater than 1.50%, the stiffness of Specimen 3 was almost the same as that of the other specimens, where the beam had undergone yielding and the inelastic deformation of the beam determined stiffness. In contrast to Specimen 3, the stiffness for Specimen 1 at a drift ratio above 2.5% tended to decrease compared to the other specimens and the decrease increased after exceeding a drift ratio of 4.0%. The decrease in stiffness was due to significant local buckling in Specimen 1 compared to the other specimens, which started when the drift ratio was greater than 2.5%. This shows that the detailing with ABP and EBF in Specimens 2 and 4 could prevent significant local buckling in the final stages of loading.

4.4   Energy Dissipation Capacity

The energy dissipation capacity was evaluated by comparing the area of the load hysteresis curve versus the displacement that formed in each cycle. A comparison of cumulative dissipation energy for each specimen can be seen in Figure 9.
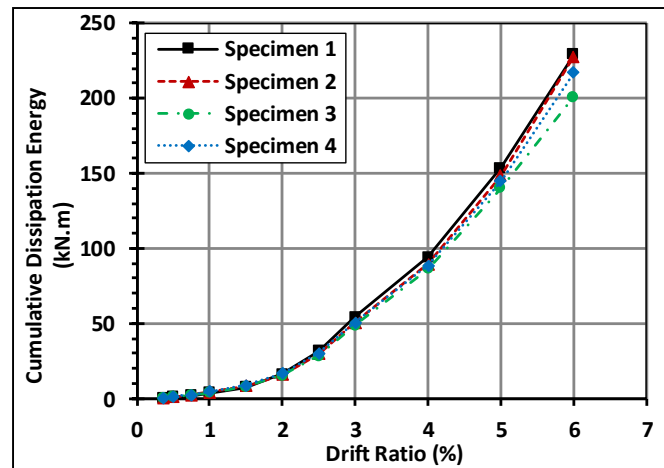

Figure 9   Cumulative energy dissipation versus drift ratio.

It can be seen that the energy dissipation of Specimens 1 and 2 was relatively the same for each loading cycle, with the difference in total dissipation energy only 0.59%. Meanwhile, Specimens 3 and 4 had lower cumulative energy dissipation than Specimens 1 and 2. Specimen 3 had the lowest cumulative energy dissipation when compared to the other three specimens. However, the energy dissipation of all specimens was almost the same up to 4.0% drift ratio.

Differences began to occur at drift ratios above 4.0% due to a beam yield mechanism and cracks in the joint panel. The energy dissipation capacity of each specimen is relevant to the level of damage that occurs in the joint panel so that

the panel distortion that causes pinching on the hysteresis curve plays a significant role in the energy dissipation capacity. Figure 5 shows the hysteresis curves of Specimens 3 and 4, which had significant pinching compared to Specimens 1 and 2. Specimen 3 had more significant pinching than the other specimens so that its energy dissipation capacity was the lowest, as confirmed by the level of damage to the joint panel, as shown in Figure 6, which was significant.

4.5   Story Drift Components

Three significant mechanisms contribute to the total story drift in the sub-assemblage specimen, including (1) beam rotation; (2) column deformation; and (3) joint shear distortion. The contribution of these deformation components to the total story drift for each specimen is shown in Figures 10 to 13.
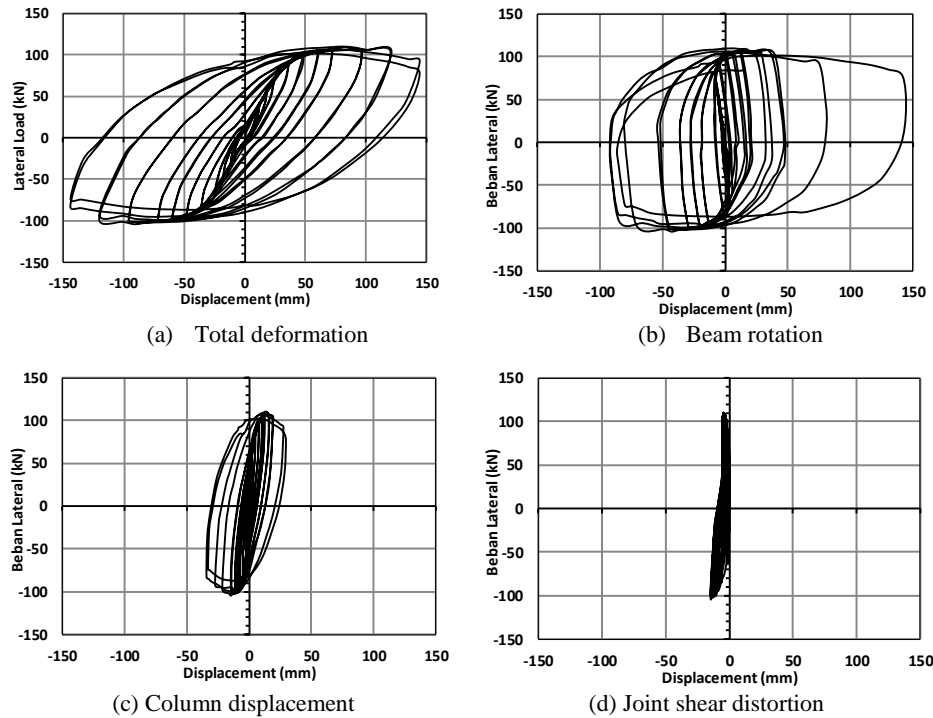

(a)   Total deformation

(b)   Beam rotation

(c) Column displacement

(d) Joint shear distortion

Figure 10   Differences in deformation components for Specimen 1.

The contribution of beam rotation was very dominant in Specimens 1 and 2, whereas the contribution of joint shear distortion was insignificant. However, the contribution of joint shear distortion for Specimen 1 was smaller than for Specimen 2. This shows that the void web on Specimen 2 did not have a

significant effect on increasing the joint shear deformation. A low to medium level of damage occurred in both specimens due to shear cracking in the joint concrete panel. Plastic hinges were formed at the beam end on the face of the column, resulting in local buckling at the flange and web of the beam, which occurred at drift ratio above 4.0%.
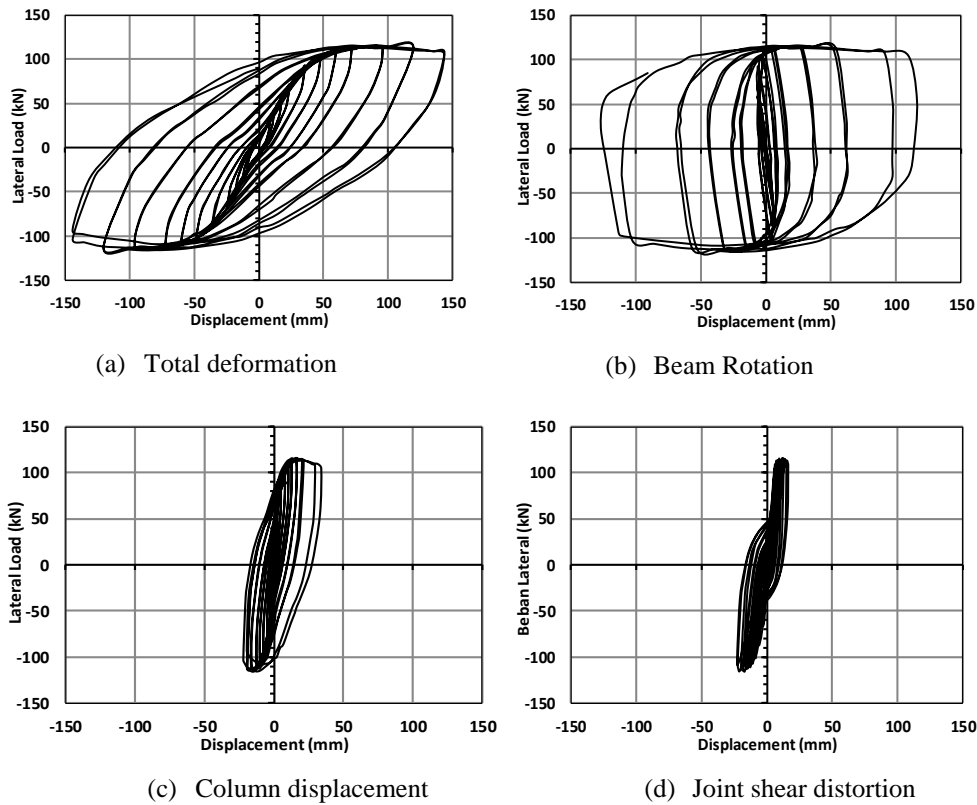

(a) Total deformation

(b) Beam Rotation

(c) Column displacement

(d) Joint shear distortion

Figure 11   Differences in deformation components for Specimen 2.

Different from Specimens 1 and 2, pinching occurred in the hysteresis curve of load versus deformation of Specimens 3 and 4, as shown in Figures 12(a) and 13(a). Figures 12(d) and 13(d) show that the pinching was due to large joint shear deformation, which was greater than in Specimens 1 and 2. In addition, by comparing the joint shear deformation of Specimens 3 and 4, in Specimen 3 it was much larger, which was confirmed by the significant level of damage at the connection concrete panel of Specimen 3 at the end of the test, as shown in Figure 6.

This shows that the combination of EBP and ABP components in the specimen with a void web effectively reduced the shear distortion of the connection. Otherwise, the specimens with only an ABP component were not able to provide confinement to the outer joint panel, causing significant shear distortion. In addition, the slip between the outer concrete panels and ABP caused even more significant distortion.

The difference between Specimen 4 and Specimen 2 was in the stirrup volumetric ratio in the joint panel, where the ratio of stirrup volume to joint volume in Specimen 2 was 1.5% and was reduced in Specimen 4 to 0.28%. By comparing these two specimens it could also be identified that a stirrup volumetric ratio of 1.5% is sufficient to provide confinement to the concrete panels in the connection area and reduce the level of damage.
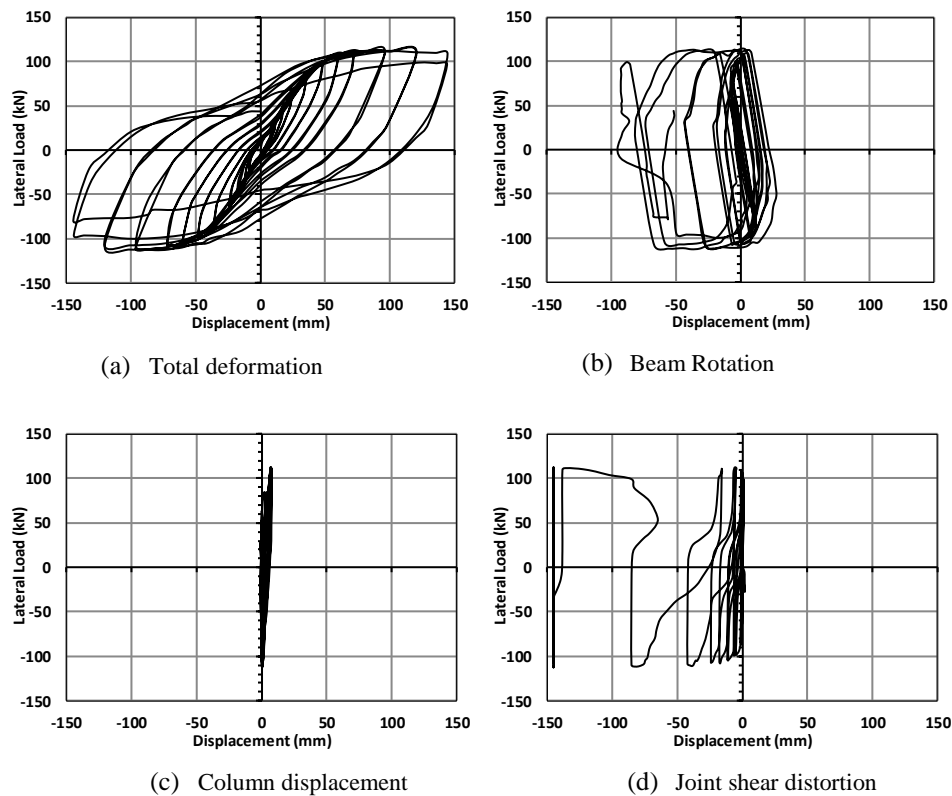

(a)   Total deformation

(b)   Beam Rotation

(c)   Column displacement

(d)   Joint shear distortion

Figure 12   Differences in deformation components for Specimen 3.

(a) Total deformation

(b) Beam rotation

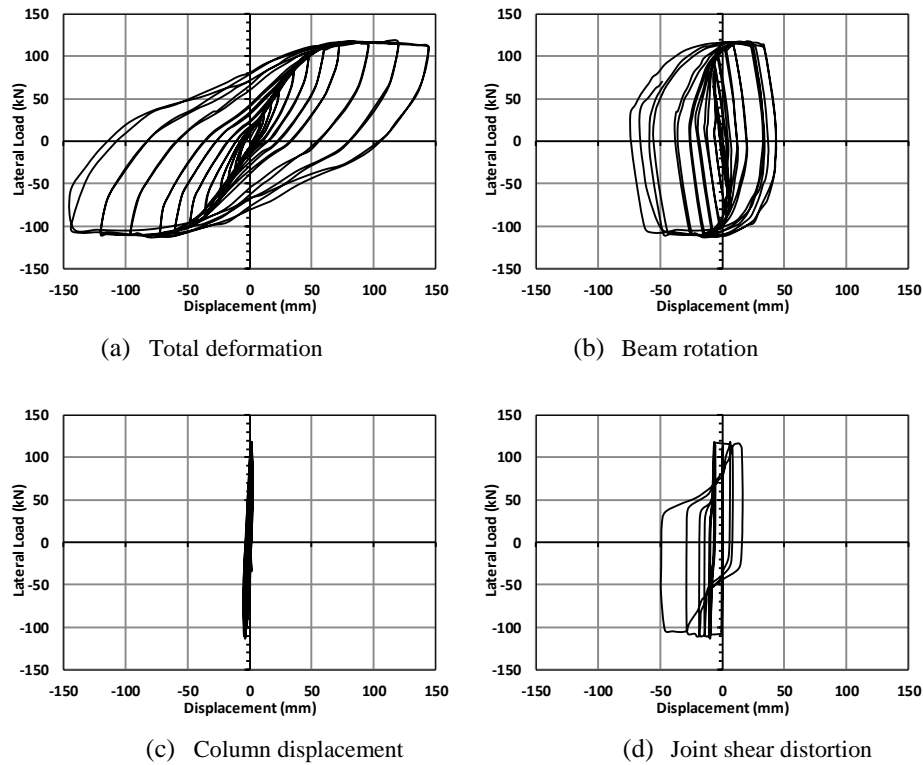(c) Column displacement

(d) Joint shear distortion

Figure 13   Differences in deformation components for Specimen 4.

5   Conclusion

The experimental results showed that all specimens had ductile behavior and were able to maintain their strength at a large story drift (> 0.004 rad) without significant loss of stiffness so the system can be used in high seismic zones. The combination of additional bearing plates (ABP) and extended band plates (EBP) in the joint with a void web was able to withstand joint shear deformation exceeding 0.01 rad with only low to medium levels of damage. EBP was proven to be very effective in providing confinement and reducing the level of damage in the joint panel. The existence of a void web did not reduce the joint shear strength, however, an increase of 4% to 12% in strength occurred compared to the specimens without void web.

The diagonal compressive strut of inner and outer concrete on the joint panel was more effective in providing joint shear resistance. Detailing with EBP and ABP in the RCS joint could reduce local buckling of the beams in the plastic zone and prevent strength degradation that occurred at drift ratios above 4.0%. A ratio of

hoop volume to joint volume of 1.50% was adequate to provide confinement and contribute to the shear strength of the RCS joint with ABP, EBP and void web. Based on the observations when casting specimens in a laboratory, a void web can improve constructability, especially for precast construction.

Acknowledgements

References

[1]   Sheikh, T.M., *Moment Connections between Steel Beam and Concrete Column*, PhD dissertation, University of Texas, Austin, 1987.

[2]   Deierlein, G.G., *Design of Moment Connections for Composite Frame Structures*, PhD dissertation, University of Texas, Austin, 1988.

[3]   Sheikh, T.M., Deierlein, G.G., Yura, J.A. & Jirsa, J.O., *Beam-Column Moment Connections for Composite Frames: Part 1*, Journal of Structural Engineering, ASCE, **115**(11), pp. 2858-2876, Nov. 1989.

[4]   Deierlein, G.G., Sheikh, T.M., Yura, J.A. & Jirsa, J.O., *Beam-Column Moment Connections for Composite Frames: Part2*, Journal of Structural Engineering, ASCE, **115**(11), pp. 2877-2896, Nov. 1989.

[5]   ASCE Task Committee on Design Criteria for Composite Structures in Steel and Concrete, *Guidelines for Design of Joints between Steel Beams and Reinforced Concrete Columns*, ASCE Journal of Structural Engineering, **120**(8), pp. 1330-2357, 1994.

[6]   Cordova, P.P., Deierlein, G.G., *Validation of the Seismic Performance of Composite RCS Frames: Full-Scale Testing, Analytical Modeling, and Seismic Design*, Report No. 155, The John A. Blume Earthquake Engineering Center, Department of Civil and Environmental Engineering, Stanford University, Sept 2005.

[7]   Alizadeh, S., Attari, N.K.A. & Kazemi, M.T., *Experimental Investigation of RCS Connections Performance Using Self-Consolidated concrete*, Journal of Constructional Steel Research, **114**, pp. 204-216, 2015.

[8]   ACI 316M-14, *Building Code Requirements for Structural Concrete*, Reported by ACI Committee, **318**, 2014.

[9]   ANSI/AISC 341-16, *Seismic Provision for Structural Steel Building, American Institute of Steel Construction*, 2016.

[10]   ASTM A572/A572M-12, *Standard Specification for High-Strength Low-Alloy, Columbium-Vanadium Structural Steel*, 2012.

[11]   Liang, X. & Parra-Montesinos, G., *Seismic Behavior of Reinforced Concrete Column-Steel Beam Subassemblies and Frame Systems*, Journal of Structural Engineering, ASCE, 2004.

[12]   ACI 374.2R-13, *Guide for Testing Reinforced Concrete Structural Elements Under Slowly Applied Simulated Seismic loads*, Reported by ACI Committee, **374**, 2013.